Current Research in Food Science 9 (2024) 100856

Contents lists available at ScienceDirect

Current Research in Food Science

journal homepage: www.sciencedirect.com/journal/current-research-in-food-science

Influence of electrohydrodynamics on the drying characteristics, microstructure and volatile composition of apricot abalone mushroom (*Pleurotus eryngii*)

Peng Guan [a], Changjiang Ding [a,b,*], Jingli Lu [a,**], Wurile Bai [a], Jiaqi Liu [a], Junjun Lian [b], Zhiqing Song [b], Hao Chen [a], Yun Jia [a]

[a] College of Science, Inner Mongolia University of Technology, Hohhot, 010051, China
[b] College of Electric Power, Inner Mongolia University of Technology, Hohhot, 010051, China

ARTICLE INFO

Handling Editor: Dr. Maria Corradini

Keywords:
Electrohydrodynamics (EHD) drying
Apricot abalone mushroom
Volatile profiles
Low-field nuclear magnetic resonance (LF-NMR)
Microstructure
Food quality

ABSTRACT

The study explored the use of current fluid dynamics drying technology for apricot abalone mushroom, examining how different output voltages (15, 25, and 35 kV) affected drying characteristics, microstructure, and volatile components. Comparisons were made with samples dried using hot air drying (HAD) and natural air drying (AD). Results revealed that HAD had the fastest drying rate at 0.29664($g{\cdot}h^{-1}$). However, apricot abalone mushroom treated with electrohydrodynamic drying (EHD) maintained a color closer to fresh samples, exhibited a 21% increase in the ordered structure of protein secondary structure, a 12.5-fold increase in bound water content, and the most stable cell structure compared to HAD and AD treatments. A total of 83 volatile organic compounds were identified in the apricot abalone mushroom, with alcohols and aldehydes being the most prominent in terms of threshold and relative content, peaking in the 35 kV treatment group. These findings provide both experimental and theoretical insights into applying current fluid dynamics for drying apricot abalone mushroom.

1. Introduction

Apricot abalone mushroom (*Pleurotus eryngii*) is a widely consumed edible with a unique flavor and several health-promoting benefits. Many studies reported that bioactive fractions isolated from apricot abalone mushroom show a wide range of bioactive effects (Kleftaki et al., 2022; Krakowska et al., 2020). The moisture content of fresh apricot abalone mushroom is about 88%. Due to the high moisture content, apricot abalone mushroom have high respiration after picking and are highly susceptible to microbial attack and spoilage, which seriously affects the quality of fresh mushrooms (Guo et al., 2023). Due to simple operation and low price, hot air drying is widely used in the food industry, but there are shortcomings such as low energy utilization and loss of nutrients (He et al., 2023). Natural drying equipment is low-cost, but long-term exposure to the air is easily contaminated by microorganisms, thus affecting the inner nutrition of apricot abalone mushroom. Infrared drying can significantly shorten the drying time and improve product quality, but its effect is often affected by the infrared wavelength, food surface porosity and composition (Bai et al., 2023). Microwave drying is popular because of its high efficiency and high rehydration rate, but the high initial cost and uneven heating with limited microwave transmittance are persistent problems in microwave drying (Wang et al., 2024). Therefore, it is necessary to find new drying methods with low equipment cost, high drying speed, and good preservation of nutrients. The emergence of electrohydrodynamic drying (EHD) technology is a good solution to this problem (Anukiruthika et al., 2021).

EHD is a non-thermal drying technique under the synergistic effect of a non-uniform electric field and ionized air, which is very beneficial for heat-sensitive materials. The EHD drying system consists of two electrodes, a pin-plate emission electrode, and a flat-plate ground electrode. When a high voltage is applied to the needle plate electrode, the needle tip discharge is enhanced. The surrounding air is forced to ionize into a plasma consisting of OH^-, N^+, O^{2-} and other free radicals and reactive atoms (Chen et al., 2012). The motion of these ions in the presence of a non-uniform electric field produces an ionized wind (Anukiruthika et al., 2021). EHD has been widely used for drying biological materials

* Corresponding author. College of Science, Inner Mongolia University of Technology, Hohhot, 010051, China.
** Corresponding author.
E-mail addresses: ding9713@163.com (C. Ding), lujingli2004@163.com (J. Lu).

https://doi.org/10.1016/j.crfs.2024.100856
Received 29 July 2024; Received in revised form 29 August 2024; Accepted 14 September 2024
Available online 16 September 2024

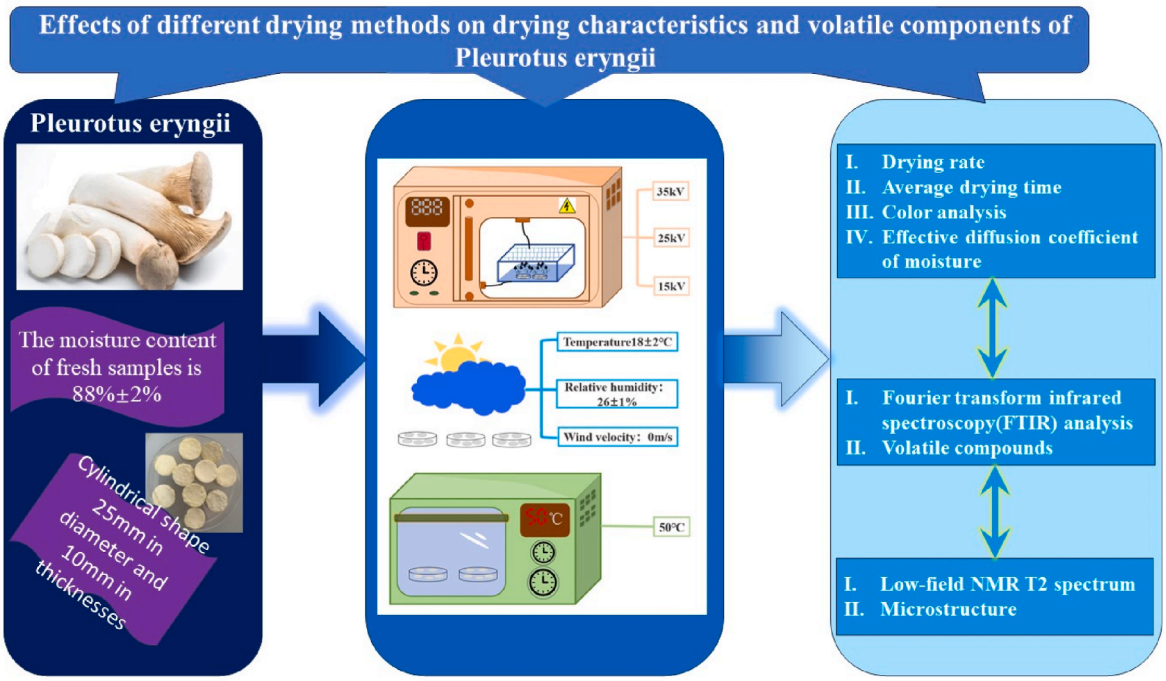

Scheme 1. Experimental flowchart.

such as *Citrus sinensis* L, pineapple, house cricket flour, and 'Ankara' pear, etc (Polat and Izli, 2022; Psarianos et al., 2024; Suvanjumrat et al., 2024; Zhang et al., 2023). Studies also showed that the cold plasma generated by the corona discharge during EHD drying has significant benefits on the quality parameters of food products such as proteins, lipids, and starches (Liu et al., 2024; Psarianos et al., 2024). However, some recent studies found that the electric field and cold plasma treatment may lead to oxidation of lipids and denaturation of proteins in food, which are important basic substances affecting flavor (Perez-Andres et al., 2018).

The odor of food is a combination of several volatile organic compounds (VOCs), and differences in the type and amount of these VOCs produce different types of aromas (Rong et al., 2023). A series of chemical reactions and various factors during the drying process led to changes in food flavor. The current study found that thermal drying is usually a combination of heat, oxygen, and various other adversity stresses to maintain quality. During this process, lipids, especially unsaturated fatty acids, are structurally very unstable and are easily deteriorated by light, heat, and oxygen and may be oxidized to aldehydes and other compounds (Ni et al., 2023). Aldehydes can further react with proteins to promote oxidative denaturation of proteins. At the same time, reactive oxygen species from protein oxidation can accelerate lipid oxidation (Huang et al., 2022). Therefore, inappropriate processing methods or conditions can lead to the destruction of nutrients such as amino acids and fatty acids in apricot abalone mushroom, thereby affecting flavor and sensory properties. However, to the best of our knowledge, most scholarly studies have focused on drying equipment and its effect on the drying characteristics of aqueous materials (Onwude et al., 2021). There are no detailed reports on the effect of EHD on volatile organic compounds during apricot abalone mushroom drying.

This study aims to systematically analyze the drying characteristics, microstructure, and volatile organic compounds of apricot abalone mushroom under different voltages. It provides a more effective drying process for the drying of plant by-products and a scientific basis for future research on volatile organic compounds in dried materials.

2. Materials and methods

2.1. Experimental materials

Fresh, intact, uniformly shaped apricot abalone mushroom of the same ripeness was purchased from a supermarket near the Inner Mongolia University of Technology in Hohhot, Inner Mongolia Autonomous Region. The fresh samples were stored in a refrigerator (HisenseBCD-197T, Beijing) at −4 °C, for no more than 3 days before the drying experiment.

2.2. EHD drying equipment

The EHD drying device mainly includes high-voltage power supply (YD (JZ)-1.5/50, Wuhan, China), adjustable controller (KZX-1.5KVA, Wuhan, China) with AC voltage range from 0 to 50 kV, and multi-needle to plate electrodes. The electrodes consist of a vertically mounted electrode with multiple sharp pointed needles projected to a fixed horizontal grounded metallic plate on which the samples to be dried was placed. The distance between the emitting point and the grounded electrode was 100 mm. The sharp pointed electrodes were connected to a power source. The distance between adjacent needles was 40 mm. The length and diameter of each needle were 20 mm and 1 mm, respectively. The grounded plate electrode was a 1000 mm × 450 mm rectangular metallic plate.

2.3. Experimental methods

The apricot abalone mushrooms were cut into cylindrical shapes with a cross-sectional diameter of 25 mm and a thickness of 10 mm. A rapid moisture detector (SH10A, Shanghai, China) was used to determine the initial moisture content of the apricot abalone mushroom, and the wet-base moisture content was measured to be 88 ± 2%. The experiment ended when the wet-base moisture content was less than 10% under the different drying conditions. The dried apricot abalone mushroom samples were analyzed for drying characteristics, infrared spectra, scanning electron microscopy (SEM), low-field nuclear magnetic resonance (NMR) T_2 spectra, and volatile organic compounds

(VOCs). The specific experimental method is shown in Scheme 1.

2.3.1. EHD drying

Voltage is an important parameter affecting the drying characteristics. The apricot abalone mushroom slices were dried under AC electric field with multiple needles-to-plate electrode at different voltages. The drying voltage was 15 kV, 25 kV and 35 kV, respectively. The ionic wind speed under different experimental conditions was measured using a thermal heat-sensitive anemometer probe. The experiments were carried out in a drying environment with a drying temperature of 18 ± 2 °C, a relative humidity of 26 ± 1%, and a wind speed of 0 m/s. Fresh apricot abalone mushroom slices were uniformly placed in the EHD system for the drying experiments.

2.3.2. AD drying

Fresh apricot abalone mushroom slices were placed in a constant temperature and humidity chamber with a temperature of 18 ± 2 °C, a relative humidity of 26 ± 1%, and an air velocity of 0 m/s.

2.3.3. HAD drying

Fresh apricot abalone mushroom slices were dried in an oven. The drying temperature was 50 °C and the drying air velocity was 2 m/s.

2.4. Moisture content

The dry basis moisture content and moisture content ratio of apricot abalone mushroom samples during drying were calculated using the following equations (Wang et al., 2017).

$$M_i = \frac{m_i - m_g}{m_g} \times 100 \tag{1}$$

$$MR = \frac{M_i\text{-}M_e}{M_0\text{-}M_e} \tag{2}$$

Where M_i is the dry basis moisture content of the apricot abalone mushroom dried to t_i time (unit: g water/g solid), m_i is the mass of the apricot abalone mushroom dried to t_i time (unit: g), m_g is the dry mass of the apricot abalone mushroom (unit: g), MR is the moisture ratio of the apricot abalone mushroom, M_e is the equilibrium moisture content of the apricot abalone mushroom, and M_0 is the moisture content of the apricot abalone mushroom at the moment t_0. Usually, the equilibrium moisture content of a food ingredient is small and negligible (An et al., 2024). Therefore, the water content equation can be simplified as:

$$MR = \frac{M_i}{M_0} \tag{3}$$

2.5. Drying rate

The drying rate is calculated as (Hu et al., 2024):

$$DR = \frac{M_t - M_{t+\Delta t}}{\Delta t} \tag{4}$$

where DR is the drying rate (unit: g water/g solid·h^{-1}), M_t is the dry basis moisture content of apricot abalone mushroom at time t, $M_{t+\Delta t}$ is the dry basis moisture content of apricot abalone mushroom at time $t + \Delta t$, and Δt is the drying time of apricot abalone mushroom.

2.6. Effective diffusion coefficient of moisture

The effective diffusion coefficient of moisture was calculated using Fick's second law (El-Mesery et al., 2024).

$$\frac{dM}{dt} = D_{eff}\frac{d^2M}{dr^2} \tag{5}$$

When the drying time is long, $MR < 0.6$, the above equation can be expressed as:

$$MR = \frac{8}{\pi^2} exp\left(-\frac{\pi^2 D_{eff} t}{4L^2}\right) \tag{6}$$

where D_{eff} is the effective diffusion coefficient and L is half the thickness of the sample. The above equation can be written by taking the logarithm:

$$\ln[MR] = -\frac{\pi^2 D_{eff}}{4L^2} t + \ln\left[\frac{8}{\pi^2}\right] \tag{7}$$

2.7. Color

The surface brightness value L^*, redness value a^*, and yellowness value b^* of apricot abalone mushroom slices before and after drying were measured directly with an automated colorimeter. The instrument was calibrated with a blackboard and a whiteboard before testing, and measurements were taken from five places on the same sample. The average of the results was taken. The expression for color difference is (Zhang et al., 2024):

$$\Delta E = \sqrt{\left(L_1^* - L_0^*\right)^2 + \left(a_1^* - a_0^*\right)^2 + \left(b_1^* - b_0^*\right)^2} \tag{8}$$

Where L_0^*, a_0^*, b_0^* are the brightness, redness, and yellowness values of fresh apricot abalone mushroom slices, and L_1^*, a_1^*, b_1^* are the brightness, redness, and yellowness values of dried apricot abalone mushroom slices, respectively.

The whiteness of apricot abalone mushroom after drying is also one of the important indicators for evaluating the color of apricot abalone mushroom, and the equation for calculating whiteness can be expressed by equation (Feng et al., 2021):

$$Whiteness = 100 - \sqrt{(100 - L^*)^2 + (a^*)^2 + (b^*)^2} \tag{9}$$

Where L*, a*, and b* are the brightness, redness, and yellowness values of apricot abalone mushroom slices before and after drying, respectively.

2.8. Infrared spectral analysis (FT-IR)

Potassium bromide (130 mg) and 1.3 mg of sample (sample to potassium bromide mass ratio 1 to 100) were ground into an onyx grinding bowl to a particle size of <2 mm. The powder was pressed at a force per unit area of 8000 psi (55–69 MPa) to form transparent tablets, and the particles were analyzed by placing them in an FTIR (Nicolet6700, USA). The scanning range was 400–4000 cm^{-1}, and 32 scans were performed at 4 cm^{-1} resolution with a signal-to-manager ratio of 50,000:1 to remove water and carbon dioxide interferences to obtain the scanned spectra (Li et al., 2024). Amide I spectra in the range 1600–1700 cm^{-1} were analyzed by baseline adjustment, Gaussian back-convolution, second-order derivatives, and curve fitting using PeakFit software (San Rafael, CA, USA). Percentages of α-helix, β-sheet, β-turn, β-antiparallel, and random coil protein secondary structure compositions were calculated.

2.9. Identification of volatile compounds

The volatile organic compounds (VOCs) of dried apricot abalone mushroom products were determined by headspace gas phase solid-phase microextraction (SPME) coupled with gas chromatography-mass spectrometry (HS-SPME-GC-MS). The dried apricot abalone mushrooms were ground into powder, and 2g of the sample was firstly weighed and transferred to a 20 ml headspace vial, equilibrated at 50 °C for 15min, and subjected to solid-phase microextraction (SPME fiber: DVB/CAR/PDMS, LabTech) at 50 °C with adsorption time of 30min, and

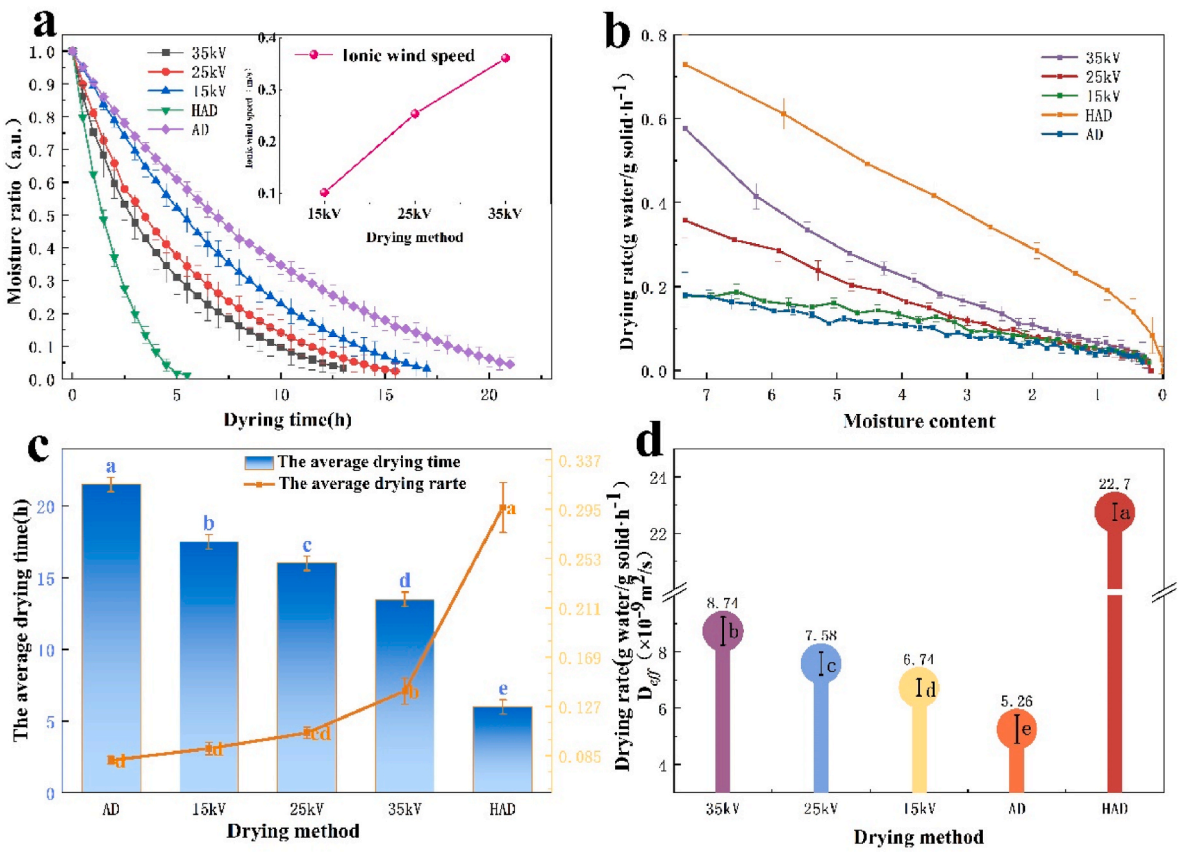

Fig. 1. Drying characteristics of apricot abalone mushroom samples under different drying methods. a: The moisture content with time and wind speed of ionized wind. b: The drying rate with the moisture content. c: Mean drying time and mean drying rate. d: Effective moisture diffusion coefficient. Note: Different letters indicate that the results are significantly different ($p < 0.05$).

desorbed at a temperature of 250 °C for 3min and then tested. A capillary column DB-5MS (Agilent, J&W Science, 30 m × 0.25 mm × 0.25 μm) was used, with an injection temperature of 250 °C, a split ratio of 10:1, a carrier gas of high-purity helium at a flow rate of 1.00 ml/min, and a starting temperature of 60 °C held for 5 min, rising to 160 °C at 6 °C/min and held for 5 min, then rising to 280 °C at 5 °C/min and held for 5 min. The temperature of the ion source was 230 °C, the temperature of the interface was 280 °C, and the scanning range was 45–450m/z. The ion source temperature was 230 °C, and the interface temperature was 280 °C. The scanning range was 45–450m/z. When volatile organic compounds (VOCs) in raw materials are determined by HS-SPME-GC-MS, the peak area is proportional to the content of VOCs, so the relative percentage content of VOCs can be obtained by semi-quantitative analysis using peak area normalization (Li et al., 2023; Zhu et al., 2021). Calculations of relative VOC content were made with reference to Quintero Ramírez et al. (2023) and Tang et al. (2023) calculations. However, some modifications were made. That is, the ratio of the peak area of each VOC to the area of the total VOC is multiplied by 100 to arrive at the relative content of the VOC (Karabagias et al., 2021).

2.10. Low-field NMR (T_2 spectrum)

Low-Field Nuclear Magnetic Resonance (LF-NMR) technique was used to determine the moisture composition and state distribution of apricot abalone mushroom slices. Apricot abalone mushroom slices treated with different voltages and drying times were placed into an NMR instrument (Bruker AVANCE III 400M, Germany) with a magnetic field strength of 0.5 T and a coil diameter of 60 mm, and a Carr-Purcell-Meiboom. The Carr-Purcell-Meiboom (CPMG) pulse sequence was used to determine the Transverse Relaxation Time of apricot abalone mushroom slices, (T_2) (Gao et al., 2009).

LF-NMR test parameters: temperature 38 °C, main frequency SF = 12 MHz, 90° pulse time P90 = 11.8 μs, 180° pulse time P180 = 19.04 μs, offset frequency O1 = 234433Hz, signal receiving bandwidth SW = 333.333 kHz, number of samples TD = 16666, relaxation decay time TW = 1500ms, accumulation number NS = 8, echo number NECH = 500, echo time TE = 0.1ms. 1500ms, accumulation number NS = 8, number of echoes NECH = 500, echo time TE = 0.1ms.

2.11. Scanning electron microscope (SEM)

Dried apricot abalone mushrooms were pasted on a sample stage with carbon conductive adhesive and sprayed with gold, and the surface structure of the dried apricot abalone mushroom was observed with a scanning electron microscope (SU8020, Japan) at 2500x and 5000x at the same position under an accelerating voltage of 10 kV.

2.12. Statistical analysis

All experiments were conducted in triplicate, with results reported as the mean ± standard deviation from these three trials. One-way analysis of variance (ANOVA) using SPSS Statistics software was performed to assess differences in drying rate, moisture content, and color data of apricot abalone mushrooms, with significance set at $p < 0.05$. Data were normalized before analysis. Infrared spectroscopy, principal component analysis (PCA), and correlated thermograms were carried out using appropriate software. The correlation between different drying methods and various metrics was analyzed, and a relevance analysis was performed to evaluate the relationship between different indices.

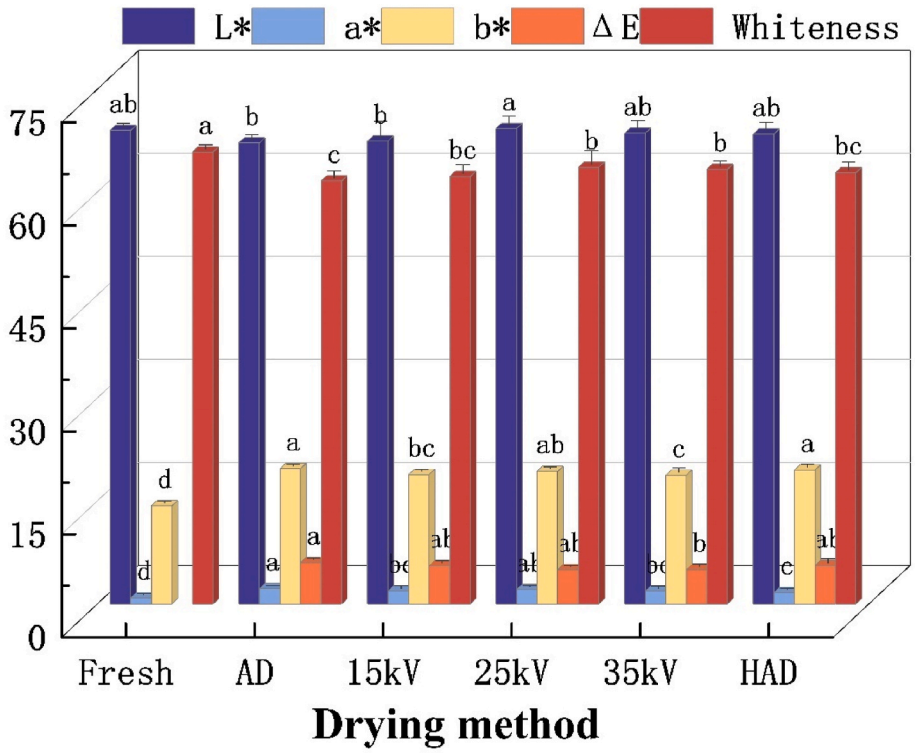

Fig. 2. Apricot abalone mushroom color under different drying methods. Where L*: brightness value; a*: redness value; b*: yellowness value; ΔE: total color difference; whiteness: whiteness value. Note: Different letters indicate that the results are significantly different ($p < 0.05$). (For interpretation of the references to color in this figure legend, the reader is referred to the Web version of this article.)

3. Results and discussion

3.1. Drying characteristics analysis

As shown in Fig. 1a, the AD experimental group had the slowest rate of decrease in water content, and the drying rate was almost constant, with an average drying rate of 0.08125($g{\cdot}h^{-1}$). The HAD experimental group had the fastest rate of decrease in water content, with an average drying rate of 0.29664($g{\cdot}h^{-1}$). The rate of reduction of water content in the EHD experimental group increased with increasing voltage, with average drying rates of 0.09116($g{\cdot}h^{-1}$), 0.1046($g{\cdot}h^{-1}$), and 0.14001 ($g{\cdot}h^{-1}$), respectively, which was consistent with the results of Xiao and Ding (2022).

HAD is characterized by high temperature, high airflow rate, thin boundary layer between the surface of the dried material and the air, and high convective heat transfer coefficient. However, high airflow and convective heat transfer coefficient can lead to rapid dehydration of the apricot abalone mushroom surface, resulting in rapid shrinkage at the beginning of drying and making it difficult for the moisture inside the apricot abalone mushroom to diffuse outward (Han et al., 2023). As a result, the drying rate of the sample increases with increasing voltage as shown in Fig. 1b. The HAD rate curve presents a high rate at high initial moisture content and decreases with decreasing moisture content. The drying process involves the evaporation of water inside the sample. In the electrohydrodynamic drying process, the movement of electrons and positive ions toward two opposite electrodes accelerates the movement of air molecules, forming an ionic wind. The ionic wind accelerates the evaporation of moisture from the surface of the apricot abalone mushroom, and this accelerates the migration of water molecules from the interior to the surface of the sample. The higher the voltage, the more obvious the promotion of the drying rate by the ionized wind. As the drying time increases, the internal moisture of the sample gradually decreases and the drying rate gradually slows down. In this way, the drying process is a deceleration period. This result corresponds to the conclusion of Iranshahi et al. (2022). Fig. 1c shows the average drying time and average drying rate of apricot abalone mushroom under different drying methods. The average drying rate of EHD drying and HAD drying was significantly higher compared to AD drying, increasing by 1.12, 1.29, 1.72 and 3.65 times, respectively, at 15 kV, 25 kV, 35 kV and HAD compared to that of AD group. The drying rate of the apricot abalone mushroom treated by EHD increased with the increase of the applied voltage, which was mainly since with the increase of the voltage, the intensity of the needle tip discharge of the upper pole plate increased, and the speed of the ionized wind increased. The ionized wind accelerated the drying rate of the material. Compared with AD, the average drying time of EHD drying and HAD drying was significantly shorter ($p < 0.05$), and the average drying time of the AD group was 1.23, 1.34, 1.59 and 3.28 times that of the 15 kV, 25 kV, 35 kV and HAD treatments, respectively.

3.2. Effective moisture diffusion coefficient (D_{eff}) analysis

Fig. 1d shows the effective water diffusion coefficient of apricot abalone mushroom under different drying methods. It can be seen that the effective water diffusion coefficient increases with increasing voltage. This trend is the same as the average drying rate, both of which are proportional to the change in ionic wind speed. The applied voltage disrupted the inner cell membrane of apricot abalone mushroom leading to the appearance of a large number of stomata, which promoted the diffusion of water molecules to the outside (Mirzaei-Baktash et al., 2022). Therefore, the faster the apricot abalone mushroom dries, the higher the effective moisture diffusion coefficient.

3.3. Color analysis

Color is closely related to food quality and is a key factor affecting consumers' first impression and recognition (Hu et al., 2024). Fig. 2 shows the changes in surface color parameters of apricot abalone

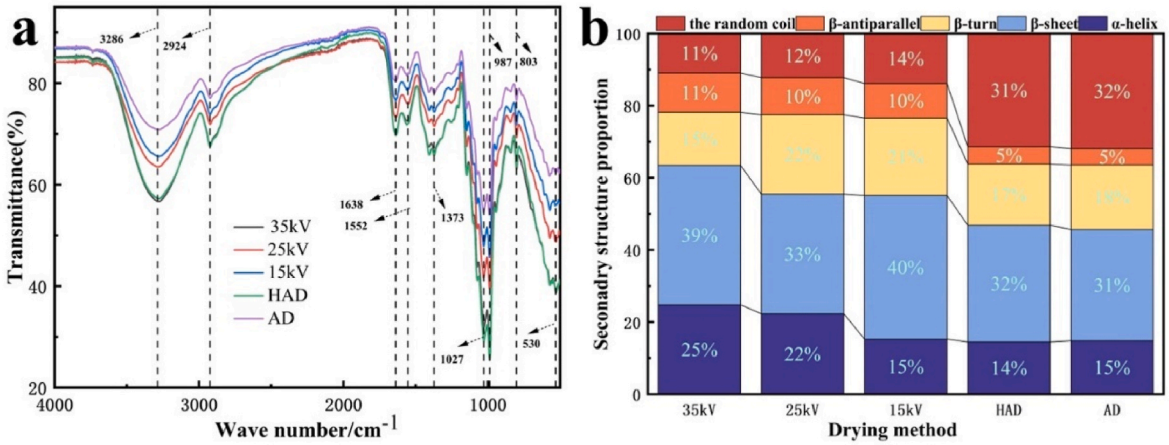

Fig. 3. Effects of different drying methods on the infrared spectra of apricot abalone mushroom and the secondary structure of proteins. a: The infrared spectra, b: The secondary structure of proteins.

mushroom before and after drying under different drying methods. The effects of different drying methods on the surface color of apricot abalone mushroom were significantly different ($p < 0.05$). The brightness value (L*) and whiteness value of apricot abalone mushroom-dried products under EHD conditions were higher than that of the products under HAD and AD conditions, and the change of ΔE was the smallest in the EHD-treated group, and it was decreased with the increase of voltage. The redness values a* of the dried apricot abalone mushroom products under different drying methods were significantly higher, with a* being the largest in AD at 2.23 ± 0.07. The reason for this phenomenon is attributed to the Meladic reaction, thermal decomposition, and non-enzymatic reaction. The apricot abalone mushrooms are rich in vitamin C and phenolics, which are chemically reacted with air when exposed to air for a long period, and the activity of polyphenol oxidase is initially drying. The polyphenol oxidase activity is elevated during initial drying, which leads to higher a* values (Sahoo et al., 2024). b* values under EHD conditions were also lower than those of both HAD and AD treatment groups, and b* values decreased with increasing voltage. Since EHD is non-thermal drying and HAD is thermal drying, this variation is mainly due to the production of enzymatic browning often found in low-temperature drying and non-enzymatic browning of phenolic compounds found in thermal drying (Fong-In et al., 2023). Enzymatic browning and color changes in fruits and vegetables are usually caused by polyphenol oxidase activity, which degrades polyphenols to colored phenols. Less color degradation in EHD can be attributed to lower PPO as well as POD activity, which can also be proof of higher antioxidant activity in EHD-dried material (Marszalek et al., 2018). The ΔE value of apricot abalone mushroom at 35 kV was the smallest, Whiteness was higher, and a* and b* lower. The smaller ΔE value indicates less browning reaction during the drying process (Wang et al., 2018), which further suggests that EHD drying can better protect the color of apricot abalone mushroom.

3.4. Infrared spectral analysis

FTIR has become a very popular technique in food science in recent years due to its unique specificity, robustness, and strong sensitivity. Fig. 3a shows the infrared spectra of dried apricot abalone mushroom products under different drying methods. It can be seen that different functional groups correspond to different characteristic absorption peaks in the infrared spectra. the peaks near 3286 cm^{-1} are broader and are mainly the N-H of proteins and the O-H telescopic vibration peaks of polysaccharides (Candoğan et al., 2020). The intensity of the energy bands (% transmittance, T) of apricot abalone mushroom dried by HAD and EHD is significantly lower than that of AD-dried apricot abalone mushroom. Zhang et al. (2016) was used in the study of polysaccharides and activity bioactivities of apricot abalone mushroom using characterization of FTIR spectral lines, also found that the typical N-H vibration near 3400 cm^{-1} overlapped with the -OH stretching vibration from 3000 to 3500 cm-1 -CH_2 stretching vibration absorption peak was observed near 2924 cm^{-1}, and the transmittance of apricot abalone mushroom increased with increasing voltage. The carbonyl C=O stretching vibration of the protein amide I group was mainly near 1638 cm^{-1}, which may also contain N-H bending vibration absorption peaks and C-N stretching vibration peaks (Li et al., 2014). The transmittance of the dried apricot abalone mushroom products under different drying methods showed a decreasing trend in the wavelength range, indicating that high-voltage drying facilitates the preservation of active components such as amide bands of amino acids and proteins, alkaloids, and unsaturated esters. Ni et al. (2020) found similar results and, suggested that the different pretreatment methods have a certain effect on the internal structure of goji and the active components. Amide II: N-H bending of proteins, C-N stretching of proteins, and C-O-H and methyl bending modes of lipids were mainly observed near 1552 cm^{-1}, COO-symmetric stretching of fatty acids and -CH_3 bending of fats were mainly observed near 1373 cm^{-1}, and at 1000 cm $^{-1}$ near the wave number range. The intensity of the characteristic peaks after drying of apricot abalone mushroom was significantly reduced under different drying methods. This indicates that the increase in voltage is unfavorable for the preservation of carbohydrates such as polysaccharides and glycosides. The characteristic peaks of fingerprints below 950 cm^{-1} are considered to be the region containing mainly the characteristic peaks of proteins, lipids, phospholipids, and nucleic acids produced by a variety of biomolecules (Candoğan et al., 2020). As can be seen in Fig. 3a, the infrared spectral peak positions of dried apricot abalone mushroom under different drying voltage treatment conditions were similar, but the intensity of the characteristic peaks was significantly different. The absorption peak intensities were in order from strongest to weakest as follows: 35 kV > HAD >25 kV > 15 kV > AD. In summary, the appropriate EHD voltage treatment conditions are more favorable for the retention of nutrients in dried apricot abalone mushroom.

Fig. 3b shows the protein secondary structure of dried apricot abalone mushroom under different drying methods. Through baseline adjustment, Gaussian inverse convolution, second-order derivatives, and curve fitting, the shapes located in the amide I band 1600-1700 cm^{-1} in the FTIR spectra can be used to determine the protein secondary structure of the dried *a*pricot abalone mushroom product. The secondary structure corresponded to different peak positions, where β-sheet appeared at 1610-1642 cm^{-1}, the random coil at 1642-1650 cm^{-1}, α-helix at 1650-1660 cm^{-1}, β -turn occurs at 1660-1680 cm^{-1}, and

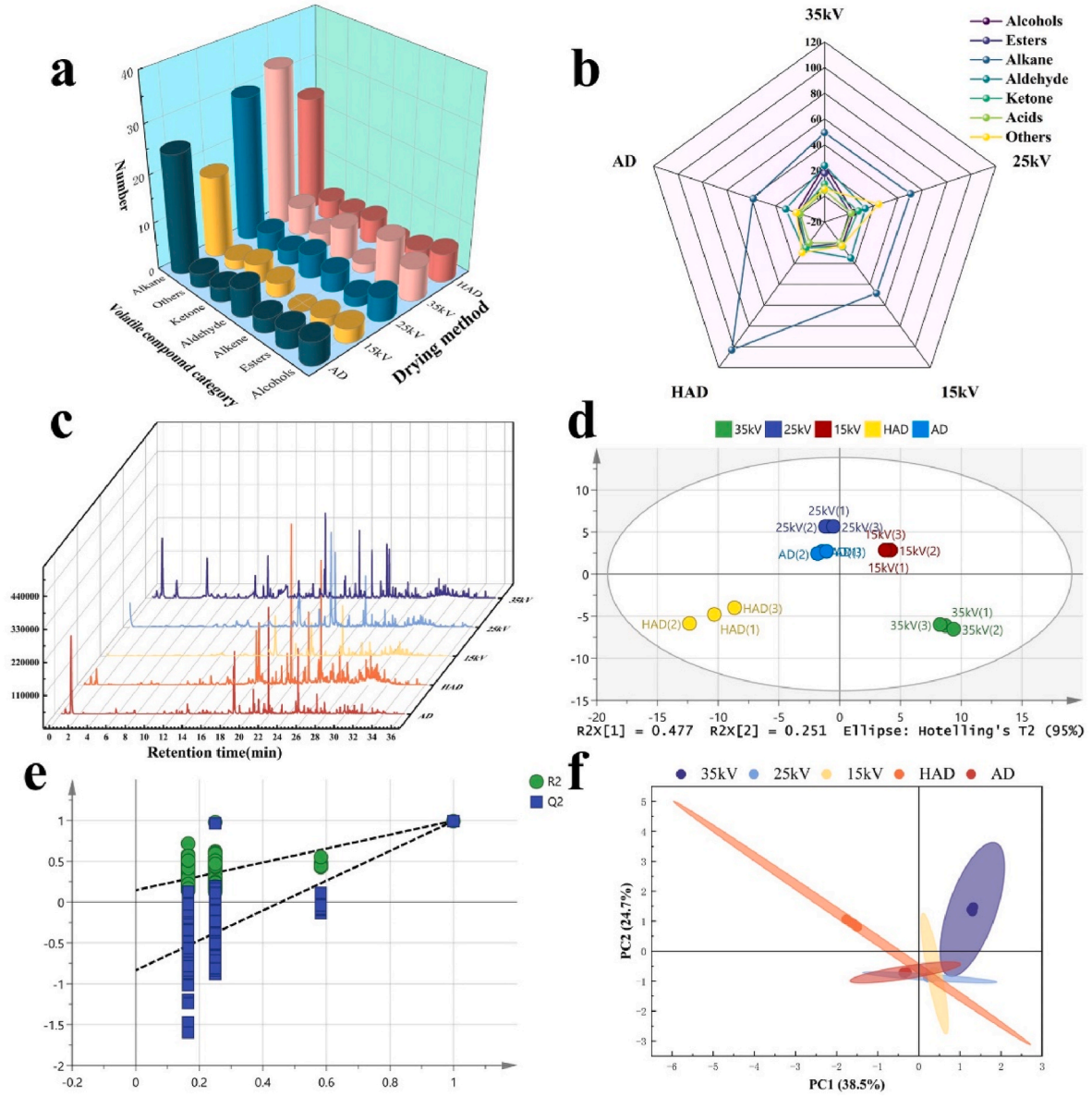

Fig. 4. Effects of different drying methods on volatile organic compounds in apricot abalone mushroom. a: The number of different species of playful organic compounds, b: The relative content of different species of volatile organic compounds, c: Fingerprints of volatile organic compounds, d: OPLS-DA, e: Results of model cross-validation, f: Principal component analysis plots of volatile organic compounds.

β-antiparallel occurs at 1680-1700 cm^{-1} (He et al., 2015). α-helix and β-sheet belong to the ordered structure, and β-turn and the random coil belong to the disordered structure (Qian et al., 2019). As shown in Fig. 3b, α-helix and β-sheets are the main forms of protein secondary structures in dried apricot abalone mushroom. It was found that β-sheets contributed most significantly to the amide I band in plant foods with high protein content (Carbonaro and Nucara, 2010). α-helix content in the 35 kV and 25 kV groups was insignificantly different, but higher than 25 kV, HAD and AD groups. β-sheets content in the 35 kV and 15 kV groups was not significantly different and higher than 15 kV, HAD and AD groups. This indicates that the protein secondary structure of apricot abalone mushroom slices treated with EHD is more stable under the appropriate voltage, and the content of β-turn and the random coil in the EHD-treated apricot abalone mushroom slices was lower than that in the HAD and AD groups, which suggested that these treatments have damaged the protein secondary structure of apricot abalone mushroom slices. This could be due to the formation due to high temperature as well as prolonged drying. Similar results were found in previous studies (Duppeti et al., 2023). In conclusion, EHD drying retained more nutrients compared to HAD drying.

3.5. *Volatile organic compound analysis*

The volatile organic compounds (VOCs) and their relative contents in apricot abalone mushroom under different drying methods were analyzed and identified by HS-SPME-GC-MS. For more convenient and intuitive observation, combined with retention index (RI) and retention time, a total of 83 volatile organic compounds were identified in the dried apricot abalone mushroom products using the NIST library, but the number of volatile organic compounds in the apricot abalone mushroom dried by different drying methods varied, with 68, 53, and 31 volatile organic compounds identified in the 35 kV, 25 kV, 15 kV, HAD and AD treatment groups, respectively, 50 and 49 volatile organic compounds. All these VOCs were categorized into 7 groups as shown in Fig. 4a–ie. 44 hydrocarbons, 11 esters, 7 aldehydes, 9 alcohols, 5 ketones, 2 acids, 5 other groups (1ether, 1phenol, 1furan, 2benzene).

Analysis of the relative content of organic compounds in different groups by peak volume normalization method revealed significant differences ($p < 0.05$) in the relative content of volatile organic compounds in 35 kV, 25 kV, 15 kV, HAD and AD samples. With the shared VOCs as the dependent variable and different drying methods as the independent variables, apricot abalone mushroom under different drying methods could be effectively distinguished by orthogonal partial least squares discriminant analysis OPLS-DA. The results in Fig. 4d showed that 25 kV, 15 kV and AD groups are located in the positive half-axis of the vertical axis, and 35 kV and HAD are located in the lower half-axis of the vertical axis. The fit index R_x^2 for the independent variable in this analysis was 0.97, the fit index (R_y^2) for the dependent variable was 0.98, and the model prediction index Q^2 was 0.974, both R^2 and Q^2 exceeded 0.5, which indicated acceptable model fit results (Chung et al., 2019). After 200 substitution tests, as shown in Fig. 4e, the intersection of the Q^2 regression line with the vertical axis is less than 0, indicating that the model is not overfitted and the model is validated. The results obtained are useful for the identification and analysis of volatile organic compounds in apricot abalone mushroom under different drying methods. Fig. 4c shows the fingerprints of volatile organic compounds in apricot abalone mushroom under different drying methods, and the graphs were established according to the parameters of peak retention time and peak area of volatile organic compounds, while the fingerprints of volatile organic compounds in apricot abalone mushroom under different drying methods were also significantly different. The contribution of odor-active compounds to the overall odor profile of food products depends not only on their concentrations but also on their thresholds (Li et al., 2024).

Fig. 4b shows the relative contents of volatile organic compound categories of dried apricot abalone mushroom products under different drying methods. The categories and contents of volatile organic compounds can be an important indicator in distinguishing apricot abalone mushroom dried under different drying methods. The above results showed that apricot abalone mushroom under different drying methods would have the loss of certain VOCs and the production of new VOCs and that there were four main ways to promote the formation of VOCs during the drying process in different drying methods, including the Meladic reaction, the degradation of long-chain compounds, the oxidization and degradation of lipids, and the interactions between amino acids (Zhang et al., 2023). The changes in VOCs are complex and will be further analyzed later for various types of VOCs.

Alcohols have a high threshold, usually with specific floral and fruity aromas (Yun et al., 2021), and are mainly produced by the reduction of the corresponding aldehydes as well as by oxidative decomposition of lipids (Zhang et al., 2019). Alcohol volatiles determined by gas chromatography-mass spectrometry (GC-MS) were highest in the 35 kV group. The highest content of alcohol volatiles from apricot abalone mushroom under different drying methods were 1-Hexanol and 1-Octen-3-ol, where 1-Hexanol behaves as a clear colorless liquid and the compound has the flavor of Banana, Flower, Grass, and Herb; whereas, 1-Octen-3-ol is allyl alcohol also known as mushroom alcohol is a compound that is found in many mushrooms and fungi in the main volatile organic compounds, colorless oily liquid, rich sweet earthy odor with a strong herbal aroma. With the increase of voltage 1-Hexanol and 1-Octen-3-ol content increased significantly, both greater than the AD and HAD groups. The HAD group content was the lowest indicating that high temperature exacerbates the loss of alcohol volatiles which is consistent with the results of (Hu et al., 2024).

Aldehydic volatiles exhibit a low threshold and a strong aroma-enhancing capacity, contributing significantly to the odor, and they are formed mainly through lipid oxidative degradation and Meladic reactions (Ni et al., 2023). A total of seven aldehyde volatiles were identified under different drying methods, of which the most important compounds were Nonanal, Benzaldehyde, Benzeneacetaldehyde, and 2-Nonenal, (E)-. Nonanal is a clear brown liquid with a rose and orange aroma. colorless to yellow liquid with a bitter almond odor. Benzeneacetaldehyde is a colorless to slightly yellow oily liquid with hyacinth and lilac flavors and a penetrating, pungent floral and sweet aroma.2-Nonenal, (E)- is a white to slightly yellow liquid with a penetrating, fatty, violet aroma. The aldehydic volatiles were higher in the EHD group than in the AD and HAD groups. This suggests that aldehydes are better retained under low temperature and high voltage conditions, while high-temperature conditions are unfavorable for the formation of aldehyde volatiles. The same results were obtained with (Zhang et al., 2023). Interestingly, the highest content of aldehyde volatiles was Nonanal, which was the highest in the 15 kV treatment group, suggesting that choosing the right voltage will have better retention of some aldehyde volatiles.

A total of 11 ester volatiles were identified in dried apricot abalone mushroom products under different drying methods. Esters usually originate from esterification reactions between alcohols and acids caused by degradation of fats or proteins, or from alcoholysis of triglycerides, fatty acids, and esters in ethanol (Yun et al., 2021). Most esters have a fruity flavor. Propanoic acid, propyl ester, Hexanoic acid, hexyl ester, and Formic acid, octyl ester are ester volatiles with high content in apricot abalone mushroom under different drying methods. All of them are colorless transparent liquids with fruity aromas. The prolonged sunlight and high temperature in natural drying and hot air drying were detrimental to the retention of esters, combined with the highest content of lipid volatiles in the 35 kV treatment group in Fig. 4b. This finding verified the conclusion of Zhang et al. (2024).

Hydrocarbons have little effect on the volatile flavor of apricot abalone mushroom as a whole due to their high thresholds and can act as harmonizers between the various volatile components. However, some alkanes have unique flavors, such as D-Limonene detected in HAD, which can give a fresh orange aroma and lemon aroma to food products.

Ketone volatiles usually originate from lipid oxidation, alkane degradation, and Meladic reactions. Although the content of ketone volatile organic volatiles in apricot abalone mushroom is low under different drying methods, they still produce butter and blue cheese flavors in dried apricot abalone mushroom products (Bi et al., 2023). The highest content is 2-Undecanone,2-Undecanone is a colorless to pale yellow liquid with a citrus, fatty, ruey flavor. Acids are produced by the catabolism of carbohydrates, and acid volatiles are the least volatile compounds in apricot abalone mushroom, with only two. Pentanoic acid, 2-methyl-, and Pentanoic acid, 2-methyl-, and anhydride, respectively. Pentanoic acid, 2-methyl-, is a branched-chain saturated fatty acid, a colorless to pale yellow liquid with a caramelized taste and an irritating odor, and is present only within the EHD treatment group. The content increased with increasing voltage. Pentanoic acid, 2-methyl-, anhydride is a colorless liquid with an irritating odor. Both acid volatiles were highest in the 35 kV group, and EHD had a good retention effect on the acids. In addition, GC-MS detected some other volatile constituents of apricot abalone mushroom under different drying methods. Butylated Hydroxytoluene is a white, crystalline, or flaky solid, odorless, or with a characteristic faint aromatic odor. Butylated Hydroxytoluene is one of the most commonly used antioxidants and is recognized as safe for use in fat-containing foods, pharmaceuticals, petroleum products, rubber, and petroleum industries (Krakowska et al., 2020). The formation of 2-pentylfuran from linoleic acid and other n-6 fatty acids with a low threshold and plant aroma has also been examined (Wall et al., 2019). It has been found that 2-pentylfuran exhibits a variety of beneficial effects such as anti-microbial, analgesic, anti-mutagenic, anti-platelet, anti-allergic, cough suppressant, anti-inflammatory and antioxidant properties and is found to be EHD > AD > HAD in terms of content (Sun et al., 2023). Phenol, 2,4,6-tris(1, 1-dimethylethyl)- present as a yellowish solid powder only in the EHD treated group. It showed that EHD treatment had a good retention effect on volatile organic compounds such as 2-pentylfuran.

Variable Importance for the Projection (VIP) reflects the variable of the OPLS-DA model, i.e., the extent to which the relative content of each substance contributes to the overall flavor and a VIP value ≥ 1 is

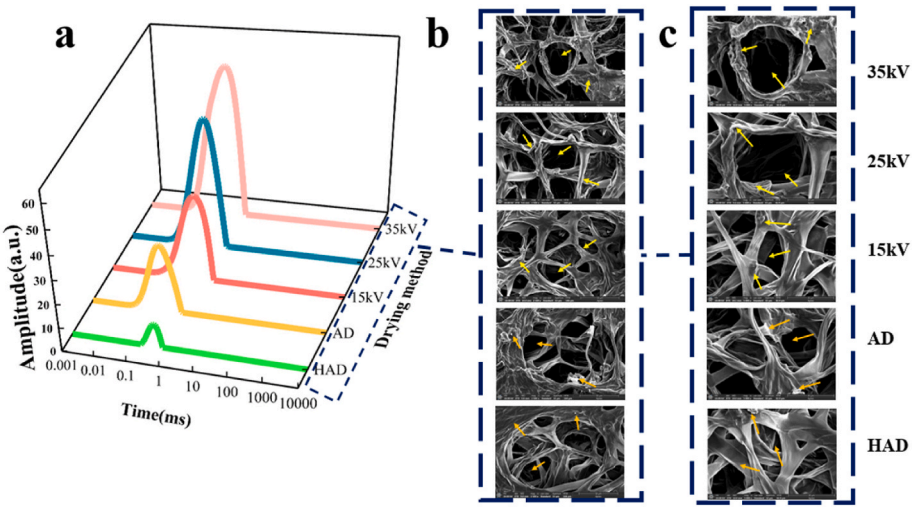

Fig. 5. Effect of different drying methods on low-field NMR and SEM images of apricot abalone mushroom. a: Low-field NMR T_2 spectrum, b: Scanning electron microscope (SEM) magnification at 2500×, c: Scanning electron microscope (SEM) images at 5000× magnification.

considered to be a significant contribution to the overall flavor, based on which differential identity markers were screened (Zhang et al., 2019), and only those volatile organic compounds with a VIP value ≥ 1 were analyzed. Only volatile organic compounds with VIP ≥1 were analyzed. A total of 20 differential characterization markers were screened according to the criterion of VIP value ≥ 1, including 3 alcohols, 2 esters, 8 hydrocarbons, 4 aldehydes, 1 ketone, 1 acid, and 1 other. Among them, 1-Hexanol, Nonanal, 1-Octen-3-ol, 2-Undecanone, Pentanoic acid, 2-methyl-, Benzaldehyde, 2-Nonenal, (E)-, and Benzeneacetaldehyde were relatively high in content of larger odor respectively.

Principal component analysis, (PCA) is widely used as a multivariate statistical analysis technique for inter-sample variation analysis, which simplifies the data and reveals the interrelationships between different samples; this analysis involves describing unsupervised classification trends between samples (Wang et al., 2024). Fig. 4f shows a plot of principal component analysis (PCA) analysis based on GC-MS data of apricot abalone mushroom under different drying methods. The cumulative variance contributions of PC1 (38.5%) and PC2 (24.7%) were 63.2%. Different drying methods had significant effects on the volatile organic compounds of apricot abalone mushroom. From Fig. 4f, it is clear that the samples of the EHD treatment group were located in the first and second quadrants, and the samples of the HAD treatment group were located in the third quadrant, which may be due to the difference between low-temperature drying and high-temperature drying. The PCA was effective in distinguishing between EHD and HAD.

3.6. *Low-field NMR (T_2 spectrum) analysis*

The relaxation time T_2 reflects the chemical environment of the hydrogen proton, which is related to the binding force and degree of freedom of the hydrogen proton (Su et al., 2020). The larger the binding force or smaller the degree of freedom of the hydrogen proton, the shorter the relaxation time T_2 (Li et al., 2014). The magnitude of the signal amplitude reflects the water activity and is a dimensionless indicator. Under the same test parameters, a larger signal amplitude in the T_2 relaxation spectrum indicates a greater number of corresponding water types. Based on the relaxation time, water in apricot abalone mushroom can be categorized into three forms, including bound water ($0.1 < T_{21} < 1$ ms), fixed water ($1 < T_{22} < 10$ ms), and free water ($T_{23} >$ 10 ms), which are labeled as A_{21}, A_{22}, and A_{23} in terms of their relative signal amplitudes (Li et al., 2014; Song et al., 2017). The T_2 relaxation spectra of the three drying methods are shown in Fig. 5a. It can be seen that after drying, the free and fixed water contents of the materials corresponding to each drying method disappeared, which is the same as the results of Su et al. (2019). It indicates that drying mainly focuses on the free water in the material as well as in the cytoplasm. However, it is interesting to note that the content of bound water was different after treatment by different drying methods. The bound water content of the material dried by EHD was significantly higher than that of HAD and AD drying, and increased with increasing voltage. The lowest bound water content of the material in HAD was attributed to the fact that the high temperatures potentially promoted cellular metabolic processes, whereas the content of free water limited the metabolic activity of the cells. Thus, in the HAD process, some of the bound water of the apricot abalone mushroom was converted to free water, which was evaporated. The highest content of bound water in apricot abalone mushroom after electric field drying is since the high-energy particles generated by the ionized air of EHD drying potentially act on the water molecules in apricot abalone mushroom, increasing the polarity of the water molecules in the apricot abalone mushroom and enhancing the binding capacity of the amino, hydroxyl, and carboxyl groups in the material. This binding capacity increases with increasing voltage, promoting the formation of bound water. This also confirms that different drying techniques altered the ratio of free hydrogen ions in the material and that EHD drying acted on the surface of the material to produce a more complete cellular structure of the material. Bound water is an important part of the cell structure. High temperature disrupts the cellular structure, leading to a decrease in the bound water content (Sun et al., 2022). The results also showed that HAD disrupted the structure of the material. Therefore, EHD drying has a clear advantage in maintaining the cell structure.

3.7. *Microstructure analysis*

From Fig. 5b, it can be seen that there are many uniform small pores distributed between the cells under 2500 × , which indicates that apricot abalone mushroom is a porous structural material. Having a highly complex internal structure, it can be effectively described by the pore network modeling (PNM) method, such as pores, nodes, tunnels, etc (Zhang et al., 2020). Complex ideal structures related to water diffusion are formed during the drying process, and the diffusion process of substances inside the apricot abalone mushroom is well described using this method.

In the EHD drying treatment, the degree of cell aggregation increased and irregular pores became more numerous as the voltage increased. The inner wall of the cells of the 5000x microstructure can be seen in Fig. 5c to become gradually less smooth, which may be due to the etching effect of the ionic wind (Luan et al., 2020). The inner cell of the

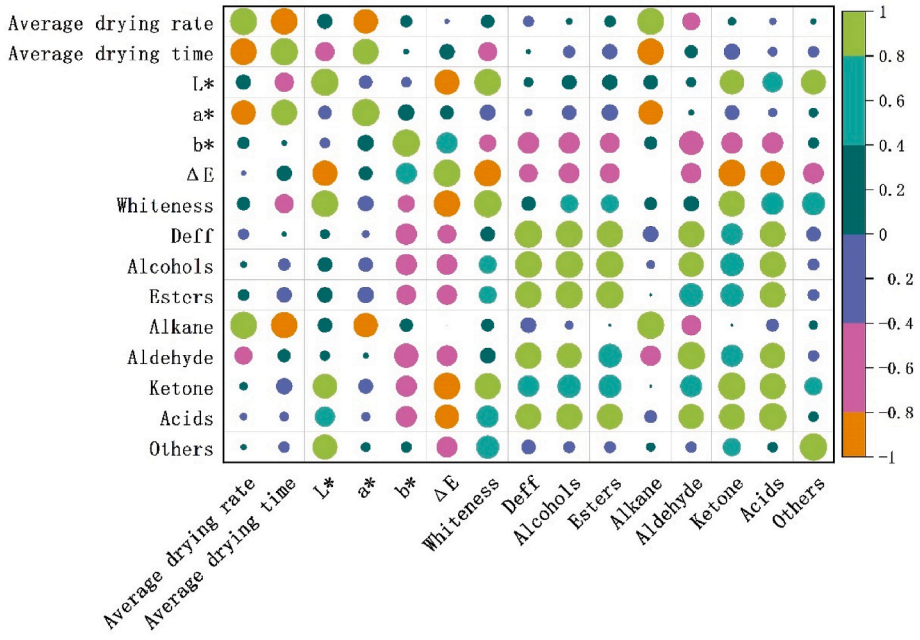

Fig. 6. Pearson correlation coefficient analysis between different drying indices.

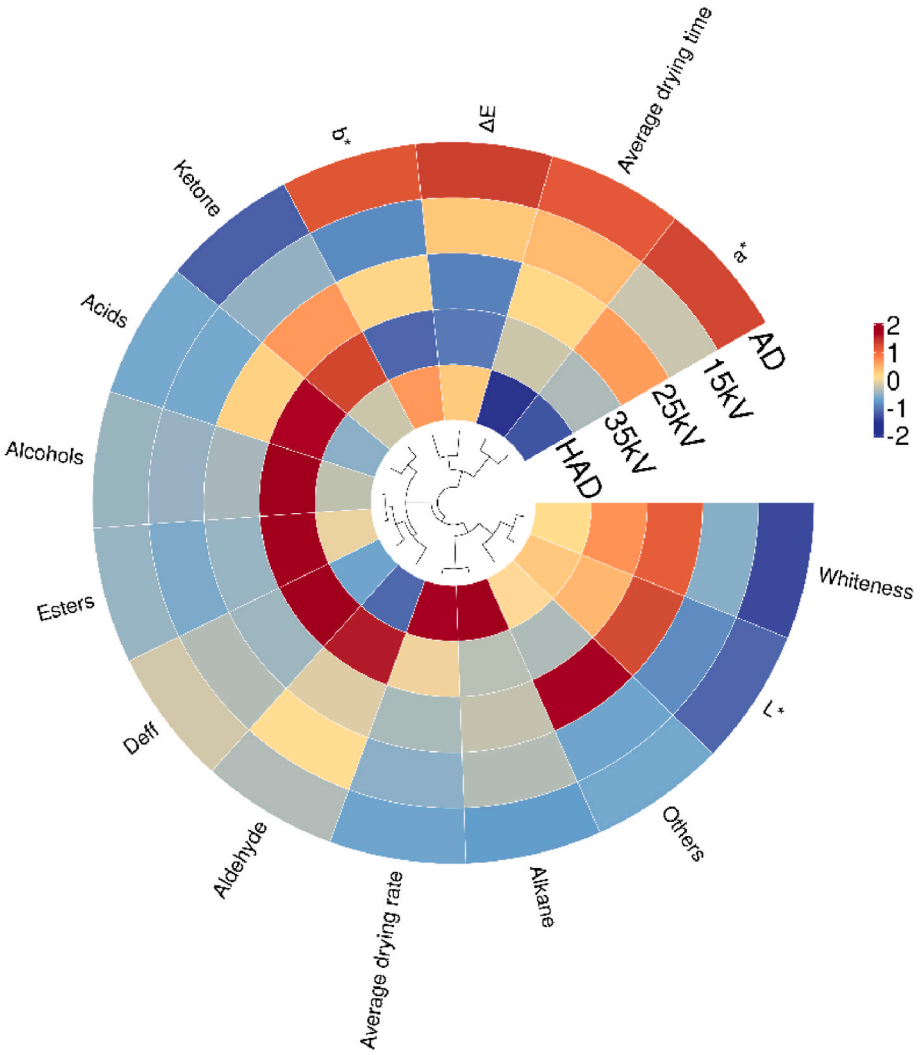

Fig. 7. Heat map relating different drying methods to drying index.

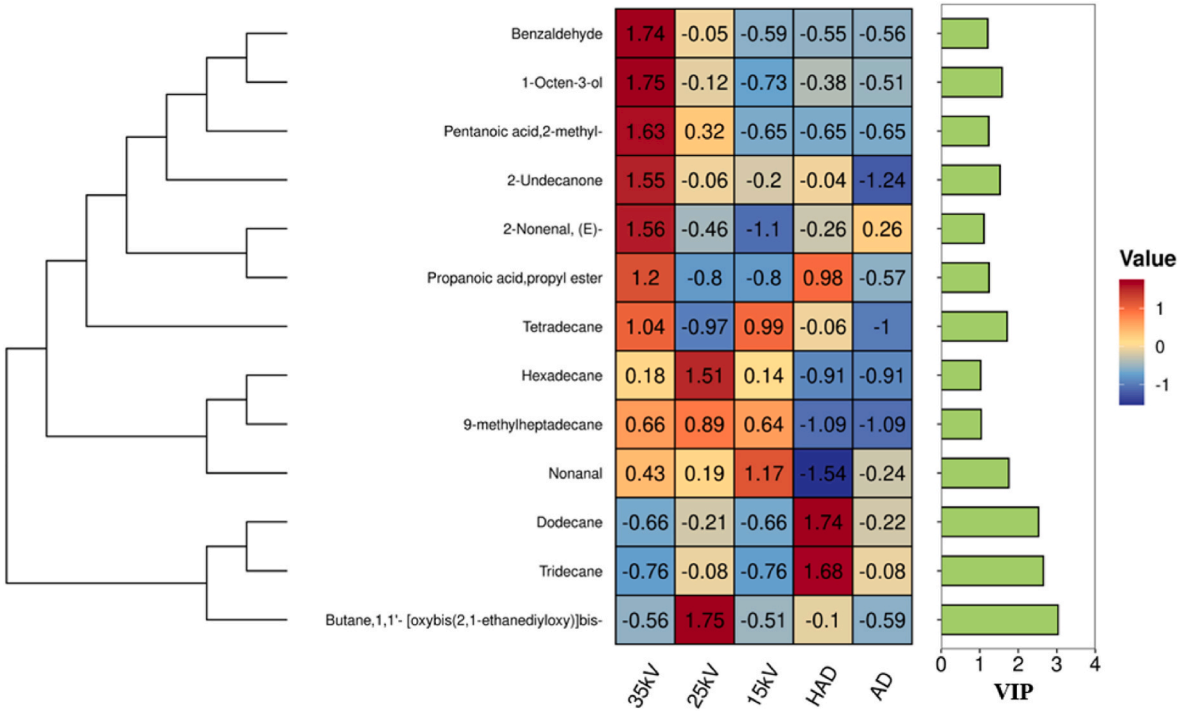

Fig. 8. Heat map of apricot abalone mushroom VOC (VIP>1) compound clustering under different drying methods.

HAD group collapsed, and the mycelium produced cross-linking and aggregation. Combined with the figure shown in Fig. 5b, it was observed that HAD effectively disrupted the skeleton, altered the cell morphology, and formed new tunnels leading to easier evaporation of water inside the cell. This is in agreement with the findings of Bai et al. (2023). The surface of the samples in the AD group appeared twisted and wrinkled. And there were irregular accumulations of lumpy or granular proteins on the surfaces of HAD and AD groups (Wu et al., 2023), further suggesting that the EHD treatment had a good retention effect on proteins. It was also noted that EHD could mitigate tissue collapse caused by prolonged hot air drying, but too high a voltage could lead to sample shrinkage and wrinkling. Specifically, the faster drying rate of HAD material is produced under conditions that destroy the surface structure of the material, which is not conducive to the production of high-quality dried apricot abalone mushroom products. Wang et al. (2024) also found that the structure of hot-air-dried apricot abalone mushroom showed varying degrees of curling, with severely twisted and distorted cells, whereas the cellular structure of EHD-dried apricot abalone mushroom was much more intact, indicating that the cells of apricot abalone mushroom dried by EHD contained more bound water than those of HAD and AD, a result that is also consistent with the conclusions reached by LF-NMR.

3.8. Statistical analysis

The experimental data (average drying rate, average drying time, color, volatile components content) were normalized and analyzed. Fig. 6 shows the Person correlation coefficient matrix. Drying rate was positively correlated with color values (L*, b*, a* and whiteness), lipids, alcohols, and ketones, while a* was negatively correlated with D_{eff}, whiteness, alcohols, lipids, alkanes, ketones, and acids. Fig. 7 shows the correlation analysis heatmap of different drying methods on the drying index. In terms of drying rate, HAD was superior to EHD. However, the results of other parameters showed that EHD was superior to HAD and AD, where L*, whiteness, effective moisture diffusion coefficient, alcohols, aldehydes, ketones, acids, and lipids were positively correlated after drying of apricot abalone mushroom in the 35 kV treatment group. Whereas, the color difference ΔE was negatively correlated. The correlation between volatiles and drying methods was also further revealed. Fig. 8 represents the relationship between 20 different volatile organic compounds (VIP>1, $p < 0.05$). The vertical axis is the 20 different volatile organic compounds and the horizontal axis indicates the different drying methods. The bar graphs demonstrated the magnitude of VIP values for the 20 volatile organic compounds. The clustering results showed that the clustering of the 20 volatile substances further revealed the correlation between different drying methods and VOCs. The positive correlation substances were most abundant in the 35 kV treatment group, further indicating that EHD drying had a better retention effect on volatile organic compounds.

4. Conclusions

Based on the research analysis, it can be concluded that different drying methods significantly impact the drying characteristics and volatile organic compounds of apricot abalone mushroom. Hot air drying (HAD) has a drying rate 2.11 times higher than electrohydrodynamic drying (EHD) and 3.65 times higher than natural air drying (AD). However, apricot abalone mushroom dried using EHD exhibit superior surface color and internal microscopic protection compared to those dried using HAD and AD. Additionally, EHD drying results in a 20% and 21% increase in the ordered structure of the protein secondary structure compared to HAD and AD, respectively. Gas chromatography-mass spectrometry (GC-MS) identified 83 volatile organic compounds in the apricot abalone mushroom. Although the types of volatile organic compounds are similar across different drying methods, EHD drying results in higher concentrations of alcohols, aldehydes, ketones, acids, furans, and other organic compounds. Notably, the threshold values and contents of 1-Octen-3-ol, 1-Hexanol, Nonanal, and 2-Undecanone are higher in EHD-dried apricot abalone mushroom, contributing to their mushroom, floral, and fatty fragrances, respectively. This research highlights EHD as a favorable drying method for apricot abalone mushroom. However, the mechanisms behind the production of volatile organic compounds remain unclear, warranting further investigation.

CRediT authorship contribution statement

Peng Guan: Writing – original draft, Methodology, Investigation, Conceptualization. **Changjiang Ding:** Writing – review & editing, Supervision, Resources, Project administration, Conceptualization. **Jingli Lu:** Writing – review & editing, Supervision, Resources, Project administration, Conceptualization. **Wurile Bai:** Visualization, Validation, Data curation, Yuting Bao, Visualization, Validation, Data curation. **Jiaqi Liu:** Visualization, Validation, Data curation. **Junjun Lian:** Visualization, Validation, Data curation. **Zhiqing Song:** Methodology, Conceptualization. **Hao Chen:** Methodology, Conceptualization. **Yun Jia:** Methodology, Conceptualization.

Declaration of competing interest

The authors declare that they have no known competing financial interests or personal relationships that could have appeared to influence the work reported in this paper.

Data availability

Data will be made available on request.

Acknowledgements

The authors are grateful for the support provided by National Natural Science Foundations of China (Nos. 12365023, 52067017 and 12265021), Program for Young Talents of Science and Technology in Universities of Inner Mongolia Autonomous Region of China (No. NJYT23020), Natural Science Foundation of Inner Mongolia Autonomous Region of China(Nos. 2022LHMS01002 and 2023LHMS05019), The Basic Scientific Research Business Project of the Universities Directly of the Inner Mongolia Autonomous Region of China (Nos. JY20220066, JY20220232, JY20240045, JY20240070 and JY20230084).

References

An, N.N., Sun, W., Li, D., Wang, L.J., Wang, Y., 2024. Effect of microwave-assisted hot air drying on drying kinetics, water migration, dielectric properties, and microstructure of corn. Food Chem. 455, 139913 https://doi.org/10.1016/j.foodchem.2024.139913.

Anukiruthika, T., Moses, J.A., Anandharamakrishnan, C., 2021. Electrohydrodynamic drying of foods: principle, applications, and prospects. J. Food Eng. 295, 110449 https://doi.org/10.1016/j.jfoodeng.2020.110449.

Bai, J.W., Wang, Y.C., Cai, J.R., Zhang, L., Dai, Y., Tian, X.Y., Xiao, H.W., 2023. Three-dimensional appearance and physicochemical properties of *pleurotus eryngii* under different drying methods. Foods 12 (10), 1999. https://doi.org/10.3390/foods12101999.

Bi, Y., Ni, J., Xue, X., Zhou, Z., Tian, W., Orsat, V., Yan, S., Peng, W., Fang, X., 2023. Effect of different drying methods on the amino acids, α-dicarbonyls and volatile compounds of rape bee pollen. Food Sci. Hum. Wellness 13, 517–527. https://doi.org/10.26599/fshw.2022.9250045.

Candoğan, K., Altuntas, E.G., İğci, N., 2020. Authentication and quality assessment of meat products by fourier-transform infrared (FTIR) spectroscopy. Food Eng. Rev. 13 (1), 66–91. https://doi.org/10.1007/s12393-020-09251-y.

Carbonaro, M., Nucara, A., 2010. Secondary structure of food proteins by fourier transform spectroscopy in the mid-infrared region. Amino Acids 38 (3), 679–690. https://doi.org/10.1007/s00726-009-0274-3.

Chen, L., Wei, Y., Zuo, X., Cong, J., Meng, Y., 2012. The atmospheric pressure air plasma jet with a simple dielectric barrier. Thin Solid Films 521, 226–228. https://doi.org/10.1016/j.tsf.2011.11.069.

Chung, I.M., Kim, J.K., Han, J.G., Kong, W.S., Kim, S.Y., Yang, Y.J., An, Y.J., Kwon, C., Chi, H.Y., Yhung Jung, M., Kim, S.H., 2019. Potential geo-discriminative tools to trace the origins of the dried slices of shiitake (*Lentinula edodes*) using stable isotope ratios and OPLS-DA. Food Chem. 295, 505–513. https://doi.org/10.1016/j.foodchem.2019.05.143.

Duppeti, H., Manjabhatta, S.N., Kempaiah, B.B., 2023. Physicochemical, structural, functional and flavor adsorption properties of white shrimp (Penaeus vannamei) proteins as affected by processing methods. Food Res. Int. 163, 112296 https://doi.org/10.1016/j.foodres.2022.112296.

El-Mesery, H.S., Qenawy, M., Li, J., El-Sharkawy, M., Du, D., 2024. Predictive modeling of garlic quality in hybrid infrared-convective drying using artificial neural networks. Food Bioprod. Process. 145, 226–238. https://doi.org/10.1016/j.fbp.2024.04.003.

Feng, Y., Xu, B., ElGasim, A.Y.A., Ma, H., Sun, Y., Xu, X., Yu, X., Zhou, C., 2021. Role of drying techniques on physical, rehydration, flavor, bioactive compounds and antioxidant characteristics of garlic. Food Chem. 343, 128404 https://doi.org/10.1016/j.foodchem.2020.128404.

Fong-in, S., Khwanchai, P., Prommajak, T., Boonsom, S., 2023. Physicochemical, nutritional, phytochemical properties and antioxidant activity of edible *Astraeus odoratus* mushrooms: effects of different cooking methods. Int. J. Gastron. Food Sci. 33, 100743 https://doi.org/10.1016/j.ijgfs.2023.100743.

Gao, S., Chapman, W.G., House, W., 2009. Application of low field NMR T2 measurements to clathrate hydrates. J. Magn. Reson. 197 (2), 208–212. https://doi.org/10.1016/j.jmr.2008.12.022.

Guo, Y., Chen, X., Gong, P., Wang, R., Qi, Z., Deng, Z., Han, A., Long, H., Wang, J., Yao, W., Yang, W., Wang, J., Li, N., 2023. Advances in postharvest storage and preservation strategies for *pleurotus eryngii*. Foods 12 (5), 1046. https://doi.org/10.3390/foods12051046.

Han, B., Ding, C., Jia, Y., Wang, H., Bao, Y., Zhang, J., Duan, S., Song, Z., Chen, H., Lu, J., 2023. Influence of electrohydrodynamics on the drying characteristics and physicochemical properties of garlic. Food Chem. X 19, 100818. https://doi.org/10.1016/j.fochx.2023.100818.

He, S., Shi, J., Walid, E., Zhang, H., Ma, Y., Xue, S.J., 2015. Reverse micellar extraction of lectin from black turtle bean (*Phaseolus vulgaris*): optimisation of extraction conditions by response surface methodology. Food Chem. 166, 93–100. https://doi.org/10.1016/j.foodchem.2014.05.156.

He, Z., Shen, Q., Wang, L., Fan, X., Zhuang, Y., 2023. Effects of different drying methods on the physical characteristics and non-volatile taste components of Schizophyllum commune. J. Food Compos. Anal. 123, 105632 https://doi.org/10.1016/j.jfca.2023.105632.

Hu, D., Yang, G., Liu, X., Qin, Y., Zhang, F., Sun, Z., Wang, X., 2024a. Comparison of different drying technologies for coffee pulp tea: changes in color, taste, bioactive and aroma components. LWT–Food Sci. Technol. 200, 116193 https://doi.org/10.1016/j.lwt.2024.116193.

Hu, J., Sun, X., Xiao, H., Liu, C., Yang, F., Liu, W., Wu, Y., Wang, Y., Zhao, R., Wang, H., 2024b. Effect of guar gum, gelatin, and pectin on moisture changes in freeze-dried restructured strawberry blocks. Food Chem. 449, 139244 https://doi.org/10.1016/j.foodchem.2024.139244.

Hu, X., Hou, Y., Liu, S., Jia, S., Zhu, Y., Lu, Y., Zhang, X., 2024c. Comparative analysis of volatile compounds and functional components in fresh and dried monk fruit (*Siraitia grosvenorii*). Microchem. J. 196, 109649 https://doi.org/10.1016/j.microc.2023.109649.

Huang, Q., Dong, K., Wang, Q., Huang, X., Wang, G., An, F., Luo, Z., Luo, P., 2022. Changes in volatile flavor of yak meat during oxidation based on multi-omics. Food Chem. 371, 131103 https://doi.org/10.1016/j.foodchem.2021.131103.

Iranshahi, K., Onwude, D.I., Martynenko, A., Defraeye, T., 2022. Dehydration mechanisms in electrohydrodynamic drying of plant-based foods. Food Bioprod. Process. 131, 202–216. https://doi.org/10.1016/j.fbp.2021.11.009.

Karabagias, I.K., Karabagias, V.K., Karabournioti, S., Badeka, A.V., 2021. Aroma identification of Greek bee pollen using HS-SPME/GC–MS. Eur. Food Res. Technol. 247 (7), 1781–1789. https://doi.org/10.1007/s00217-021-03748-4.

Kleftaki, S.A., Simati, S., Amerikanou, C., Gioxari, A., Tzavara, C., Zervakis, G.I., Kalogeropoulos, N., Kokkinos, A., Kaliora, A.C., 2022. Pleurotus eryngii improves postprandial glycaemia, hunger and fullness perception, and enhances ghrelin suppression in people with metabolically unhealthy obesity. Pharmacol. Res. 175, 105979 https://doi.org/10.1016/j.phrs.2021.105979.

Krakowska, A., Zieba, P., Wlodarczyk, A., Kala, K., Sulkowska-Ziaja, K., Bernas, E., Sekara, A., Ostachowicz, B., Muszynska, B., 2020. Selected edible medicinal mushrooms from *Pleurotus* genus as an answer for human civilization diseases. Food Chem. 327, 127084 https://doi.org/10.1016/j.foodchem.2020.127084.

Li, L., Zhang, Q., Yuan, X., Yang, H., Qin, S., Hong, L., Pu, L., Li, L., Zhang, P., Zhang, J., 2024a. Study of the molecular structure of proteins in fermented Maize-Soybean meal-based rations based on FTIR spectroscopy. Food Chem. 441, 138310 https://doi.org/10.1016/j.foodchem.2023.138310.

Li, M., Wang, H., Zhao, G., Qiao, M., Li, M., Sun, L., Gao, X., Zhang, J., 2014. Determining the drying degree and quality of chicken jerky by LF-NMR. J. Food Eng. 139, 43–49. https://doi.org/10.1016/j.jfoodeng.2014.04.015.

Li, M., Zhang, J., Li, L., Wang, S., Liu, Y., Gao, M., 2023. Effect of enzymatic hydrolysis on volatile flavor compounds of Monascus-fermented tartary buckwheat based on headspace gas chromatography-ion mobility spectrometry. Food Res. Int. 163, 112180 https://doi.org/10.1016/j.foodres.2022.112180.

Li, X., Di, T., Zhang, W., Zeng, X., Xi, Y., Li, J., 2024b. Decoding the odor profile of pea protein isolate: a multidimensional exploration based on GC-O-MS, GC × GC-O-TOF-MS, and GC-IMS. Food Biosci. 104623 https://doi.org/10.1016/j.fbio.2024.104623.

Liu, Y., Deng, J., Zhao, T., Yang, X., Zhang, J., Yang, H., 2024. Bioavailability and mechanisms of dietary polyphenols affected by non-thermal processing technology in fruits and vegetables. Curr. Res. Food Sci. 8, 100715 https://doi.org/10.1016/j.crfs.2024.100715.

Luan, X., Song, Z., Xu, W., Li, Y., Ding, C., Chen, H., 2020. Spectral characteristics on increasing hydrophilicity of Alfalfa seeds treated with alternating current corona discharge field. Spectrochim. Acta Mol. Biomol. Spectrosc. 236, 118350 https://doi.org/10.1016/j.saa.2020.118350.

Marszalek, K., Wozniak, L., Barba, F.J., Skapska, S., Lorenzo, J.M., Zambon, A., Spilimbergo, S., 2018. Enzymatic, physicochemical, nutritional and phytochemical profile changes of apple (*Golden Delicious L.*) juice under supercritical carbon dioxide and long-term cold storage. Food Chem. 268, 279–286. https://doi.org/10.1016/j.foodchem.2018.06.109.

Mirzaei-Baktash, H., Hamdami, N., Torabi, P., Fallah-Joshaqani, S., Dalvi-Isfahan, M., 2022. Impact of different pretreatments on drying kinetics and quality of button mushroom slices dried by hot-air or electrohydrodynamic drying. LWT–Food Sci. Technol. 155, 112894 https://doi.org/10.1016/j.lwt.2021.112894.

Ni, J.-B., Bi, Y.-X., Vidyarthi, S.K., Xiao, H.-W., Han, L.-D., Wang, J., Fang, X.-M., 2023. Non-thermal electrohydrodynamic (EHD) drying improved the volatile organic compounds of lotus bee pollen via HS-GC-IMS and HS-SPME-GC-MS. LWT–Food Sci. Technol. 176, 114480 https://doi.org/10.1016/j.lwt.2023.114480.

Ni, J., Ding, C., Zhang, Y., Song, Z., 2020. Impact of different pretreatment methods on drying characteristics and microstructure of goji berry under electrohydrodynamic (EHD) drying process. Innovat. Food Sci. Emerg. Technol. 61, 102318 https://doi.org/10.1016/j.ifset.2020.102318.

Onwude, D.I., Iranshahi, K., Martynenko, A., Defraeye, T., 2021. Electrohydrodynamic drying: can we scale-up the technology to make dried fruits and vegetables more nutritious and appealing? Compr. Rev. Food Sci. Food Saf. 20 (5), 5283–5313. https://doi.org/10.1111/1541-4337.12799.

Perez-Andres, J.M., Charoux, C.M.G., Cullen, P.J., Tiwari, B.K., 2018. Chemical modifications of lipids and proteins by nonthermal food processing technologies. J. Agric. Food Chem. 66 (20), 5041–5054. https://doi.org/10.1021/acs.jafc.7b06055.

Polat, A., Izli, N., 2022. Drying characteristics and quality evaluation of 'Ankara' pear dried by electrohydrodynamic-hot air (EHD) method. Food Control 134, 108774. https://doi.org/10.1016/j.foodcont.2021.108774.

Psarianos, M., Iranshahi, K., Rossi, S., Gottardi, D., Schluter, O., 2024. Quality evaluation of house cricket flour processed by electrohydrodynamic drying and pulsed electric fields treatment. Food Chem. 441, 138276 https://doi.org/10.1016/j.foodchem.2023.138276.

Qian, S., Li, X., Wang, H., Mehmood, W., Zhong, M., Zhang, C., Blecker, C., 2019. Effects of low voltage electrostatic field thawing on the changes in physicochemical properties of myofibrillar proteins of bovine *Longissimus dorsi* muscle. J. Food Eng. 261, 140–149. https://doi.org/10.1016/j.jfoodeng.2019.06.013.

Quintero Ramírez, M., Alvarez Valdez, E., Ceballos Aguirre, N., Duno, D., Taborda Ocampo, G., 2023. Volatilomic profile of the tree tomato (*Solanum betaceum Cav.*) pulp during ripening and senescence using HS–SPME with GC–MS. LWT–Food Sci. Technol. 186, 115213 https://doi.org/10.1016/j.lwt.2023.115213.

Rong, Y., Xie, J., Yuan, H., Wang, L., Liu, F., Deng, Y., Jiang, Y., Yang, Y., 2023. Characterization of volatile metabolites in Pu-erh teas with different storage years by combining GC-E-Nose, GC-MS, and GC-IMS. Food Chem. X (18), 100693 https://doi.org/10.1016/j.fochx.2023.100693.

Sahoo, M., Kumar, V., Naik, S.N., 2024. Convective drying of bitter yam slices (*Dioscorea bulbifera*): mass transfer dynamics, color kinetics, and understanding the microscopic microstructure through MATLAB image processing. Food Physics 1, 100016. https://doi.org/10.1016/j.foodp.2024.100016.

Song, Y., Zang, X., Kamal, T., Bi, J., Cong, S., Zhu, B., Tan, M., 2017. Real-time detection of water dynamics in abalone (*Haliotis discus hannai Ino*) during drying and rehydration processes assessed by LF-NMR and MRI. Dry. Technol. 36 (1), 72–83. https://doi.org/10.1080/07373937.2017.1300807.

Su, D., Lv, W., Wang, Y., Li, D., Wang, L., 2019. Drying characteristics and water dynamics during microwave hot-air flow rolling drying of *Pleurotus eryngii*. Dry. Technol. 38 (11), 1493–1504. https://doi.org/10.1080/07373937.2019.1648291.

Su, D., Lv, W., Wang, Y., Wang, L., Li, D., 2020. Influence of microwave hot-air flow rolling dry-blanching on microstructure, water migration and quality of *pleurotus eryngii* during hot-air drying. Food Control 114, 107228. https://doi.org/10.1016/j.foodcont.2020.107228.

Sun, Q., Zhang, M., Mujumdar, A.S., Yu, D., 2022. Research on the vegetable shrinkage during drying and characterization and control based on LF-NMR. Food Bioprocess Technol. 15 (12), 2776–2788. https://doi.org/10.1007/s11947-022-02917-x.

Sun, X., Yu, Y., Saleh, A.S.M., Yang, X., Ma, J., Zhang, D., Li, W., Wang, Z., 2023. Comprehensive characterisation of taste and aroma profiles of Daokou red-cooked chicken by GC-IMS and GC–MS combined with chemometrics. Int. J. Food Sci. Technol. 58 (8), 4288–4300. https://doi.org/10.1111/ijfs.16528.

Suvanjumrat, C., Chuckpaiwong, I., Chookaew, W., Priyadumkol, J., 2024. Assessment of the pineapple drying with a forced convection solar-electrohydrodynamic dryer. Case Stud. Therm. Eng. 59. https://doi10.1016/j.csite.2024.104582.

Tang, T., Zhang, M., Liu, Y., 2023. Valorization of meat and bone residue by ultrasound and high voltage electrostatic field assisted two-stage enzymatic hydrolysis: nutritional characteristics and flavor analysis. Food Biosci. 56, 103203 https://doi.org/10.1016/j.fbio.2023.103203.

Wall, K.R., Kerth, C.R., Miller, R.K., Alvarado, C., 2019. Grilling temperature effects on tenderness, juiciness, flavor and volatile aroma compounds of aged ribeye, strip loin, and top sirloin steaks. Meat Sci. 150, 141–148. https://doi.org/10.1016/j.meatsci.2018.11.009.

Wang, D.Q., Chen, X.F., Pandiselvam, R., Wang, Y., Zhao, W.P., Li, F.L., Sun, X., Guo, Y. M., Su, D.B., Xu, H.H., 2024a. Effects of microwave power control on enzyme activity, drying kinetics, and typical nutrients of Pleurotus Eryngii: exploring the blanching mechanism by microstructural and ultrastructural evaluation. J. Food Compos. Anal. 128, 106037 https://doi.org/10.1016/j.jfca.2024.106037.

Wang, J., Fang, X.M., Mujumdar, A.S., Qian, J.Y., Zhang, Q., Yang, X.H., Liu, Y.H., Gao, Z.J., Xiao, H.W., 2017. Effect of high-humidity hot air impingement blanching (HHAIB) on drying and quality of red pepper (*Capsicum annuum L.*). Food Chem. 220, 145–152. https://doi.org/10.1016/j.foodchem.2016.09.200.

Wang, J., Law, C.-L., Nema, P.K., Zhao, J.-H., Liu, Z.-L., Deng, L.-Z., Gao, Z.-J., Xiao, H.-W., 2018. Pulsed vacuum drying enhances drying kinetics and quality of lemon slices. J. Food Eng. 224, 129–138. https://doi.org/10.1016/j.jfoodeng.2018.01.002.

Wang, X., Gu, Y., Lin, W., Zhang, Q., 2024b. Rapid quantitative authentication and analysis of camellia oil adulterated with edible oils by electronic nose and FTIR spectroscopy. Curr. Res. Food Sci. 8, 100732 https://doi.org/10.1016/j.crfs.2024.100732.

Wu, D., Jia, X., Zheng, X., Mo, Y., Teng, J., Huang, L., Xia, N., 2023. Physicochemical and functional properties of Pleurotus eryngii proteins with different molecular weight. LWT–Food Sci. Technol. 184, 115102 https://doi.org/10.1016/j.lwt.2023.115102.

Xiao, A., Ding, C., 2022. Effect of electrohydrodynamic (EHD) on drying kinetics and quality characteristics of shiitake mushroom. Foods 11 (9), 1303. https://doi.org/10.3390/foods11091303.

Yun, J., Cui, C., Zhang, S., Zhu, J., Peng, C., Cai, H., Yang, X., Hou, R., 2021. Use of headspace GC/MS combined with chemometric analysis to identify the geographic origins of black tea. Food Chem. 360, 130033 https://doi.org/10.1016/j.foodchem.2021.130033.

Zhang, A.A., Ni, J.B., Martynenko, A., Chen, C., Fang, X.M., Ding, C.J., Chen, J., Zhang, J. W., Xiao, H.W., 2023a. Electrohydrodynamic drying of citrus *(Citrus sinensis L.)* peel: comparative evaluation on the physiochemical quality and volatile profiles. Food Chem. 429, 136832 https://doi.org/10.1016/j.foodchem.2023.136832.

Zhang, A.A., Xie, L., Wang, Q.H., Xu, M.Q., Pan, Y., Zheng, Z.A., Lv, W.Q., Xiao, H.W., 2024a. Effect of the ripening stage on the pulsed vacuum drying behavior of goji berry *(Lycium barbarum L.)*: ultrastructure, drying characteristics, and browning mechanism. Food Chem. 442, 138489 https://doi.org/10.1016/j.foodchem.2024.138489.

Zhang, C., Li, S., Zhang, J., Hu, C., Che, G., Zhou, M., Jia, L., 2016. Antioxidant and hepatoprotective activities of intracellular polysaccharide from *Pleurotus eryngii* SI-04. Int. J. Biol. Macromol. 91, 568–577. https://doi.org/10.1016/j.ijbiomac.2016.05.104.

Zhang, G., Wang, H., Xie, W., Wang, Q., Wang, X., Wang, C., Du, Y., Huo, C., Wang, Q., 2019a. Comparison of triterpene compounds of four botanical parts from *Poria cocos* (Schw.) wolf using simultaneous qualitative and quantitative method and metabolomics approach. Food Res. Int. 121, 666–677. https://doi.org/10.1016/j.foodres.2018.12.036.

Zhang, J., Cao, J., Pei, Z., Wei, P., Xiang, D., Cao, X., Shen, X., Li, C., 2019b. Volatile flavour components and the mechanisms underlying their production in golden pompano (*Trachinotus blochii*) fillets subjected to different drying methods: a comparative study using an electronic nose, an electronic tongue and SDE-GC-MS. Food Res. Int. 123, 217–225. https://doi.org/10.1016/j.foodres.2019.04.069.

Zhang, J., Ding, C., Lu, J., Wang, H., Bao, Y., Han, B., Duan, S., Song, Z., Chen, H., 2023b. Influence of electrohydrodynamics on the drying characteristics and volatile components of iron stick yam. Food Chem. X 20, 101026. https://doi.org/10.1016/j.fochx.2023.101026.

Zhang, J., Ding, C., Lu, J., Wang, H., Bao, Y., Han, B., Zhu, J., Duan, S., Song, Z., Chen, H., 2024b. Effects of electrohydrodynamics on drying characteristics and volatile profiles of goji berry (*Lycium barbarum L.*). LWT–Food Sci. Technol. 200, 116149 https://doi.org/10.1016/j.lwt.2024.116149.

Zhang, L., Ge, K., Wang, J., Zhao, J., Song, Y., 2020. Pore-scale investigation of permeability evolution during hydrate formation using a pore network model based on X-ray CT. Mar. Petrol. Geol. 113, 104157 https://doi.org/10.1016/j.marpetgeo.2019.104157.

Zhu, J., Niu, Y., Xiao, Z., 2021. Characterization of the key aroma compounds in Laoshan green teas by application of odour activity value (OAV), gas chromatography-mass spectrometry-olfactometry (GC-MS-O) and comprehensive two-dimensional gas chromatography mass spectrometry (GC x GC-qMS). Food Chem. 339, 128136 https://doi.org/10.1016/j.foodchem.2020.128136.